Simple Gain Probability Functions For Large Reflector Antennas Of JPL/NASA[1,2]

Vahraz Jamnejad
Jet Propulsion Laboratory
California Institute of Technology
Pasadena, CA 91109
818-354-2674
vahraz.jamnejad@jpl.nasa.gov

Abstract — Simple models for the patterns as well as their cumulative gain probability and probability density functions of the JPL/NASA Deep Space Network (DSN) antennas are developed. These are needed for the study and evaluation of interference from unwanted sources such as the emerging terrestrial system, High Density Fixed Service (HDFS), with the Ka-band receiving antenna systems in Goldstone Station of the JPL/NASA Deep Space Network.

Several different models for the high gain ground antennas of the JPL/NASA Deep Space Network (DSN) are considered. The model definitions are then used to evaluate cumulative probability functions and probability density functions for the gain values at a receiving antenna randomly located anywhere in the far field of the model antenna. Both two-dimensional models which simulate the pattern in a plane cut through the boresight of the antenna and the range of the angle from boresight to ±180 degrees and three-dimensional ones in which the pattern is given anywhere in the half-space above the ground, with the range of angle from zero at boresight to 90 degrees are considered. In both cases, regular as well as smooth "interpolated" models have been developed.

The gain value as seen by a receiver at a random location and exposed to the radiation from a transmitting antenna with a given gain profile, can be thought of as a uniformly distributed random variable. Formulas are derived and various plots are presented for the gain models and their associated cumulative probability functions and probability density functions.

TABLE OF CONTENTS

1. INTRODUCTION
2. CLOSED-FORM ANTENNA PATTERN MODELS
3. GAIN PROBABILITY FUNCTIONS
4. SUMMARY AND CONCLUSIONS

1. INTRODUCTION

There is a growing concern that emerging terrestrial systems, such as High Density Fixed Service (HDFS), may interfere with the Ka-band receiving antenna systems in Goldstone Station of the JPL/NASA Deep Space Network [1,2]. In this scenario a large number of microwave transmitters will be installed in large urban centers in the future to provide high-density fixed services (HDFS). The frequency band proposed for use by these transmitters overlaps the Ka-band (27-40 GHz) allocated for NASA's Deep Space Network (DSN) receivers. Interference signals from these transmitters can propagate over the horizon and interfere with the DSN through various mechanisms, such as ducting, rain scattering, and diffraction. Both the present 34-meter antennas which are equipped with Ka-band feeds, as well the 70-meter antennas which might be outfitted to provide receive capabilities in the future will be affected by the HDFS interference. In support of the study of this interference, simple models for the patterns of the DSN antennas as well as their cumulative gain probability functions and probability density functions will be required. This study will also be helpful in many similar cases such as those outlined in [3,4].

Here, we first consider several different models for the high gain ground antennas of the JPL/NASA Deep Space Network (DSN). The model definitions are then used to evaluate cumulative probability functions and probability density functions for the gain values at a receiving antenna randomly located anywhere in the far field of the model antenna. The models are all assumed to be circularly symmetric around the boresight axis. We distinguish two cases for the gain models. A two-dimensional case, in which the model simulate the pattern in a plane cut through the boresight of the antenna and the range of the angle from boresight is assumed to be from zero to 180 degrees. A three-dimensional case, in which the pattern is given anywhere in the half-space above the ground, and the range of the angle from boresight is assumed to be from zero to 90 degrees. In both cases, regular as well as smooth "interpolated" models have been developed.

The gain value as seen by a receiver at a random location, exposed to the radiation from a transmitting antenna with a given gain profile, can be thought of as a uniformly distributed random variable. Formulas are derived and various plots are presented for the gain models and their

[1] 0-7803-7651-X/03/$17.00 © 2003 IEEE
[2] IEEEAC paper #1339, Updated Jan. 09, 2003

associated cumulative probability functions and probability density functions. The probability density functions for the non-interpolated models have impulse responses both at the beginning and the end points for both the 2-D as well as 3-D cases. In the interpolated cases, however, there are no impulse functions, but the function goes to infinity at both the beginning and end points for the 2-D cases, and only at the beginning points for 3-D cases.

2. CLOSED-FORM ANTENNA PATTERN MODELS

Actual and realistic patterns involve many factors, too complicated and diverse, to be exactly accounted for in a simple theoretical computation. For example, the position of nulls and peaks in the sidelobe regions vary as a function of antenna gravitational loading, winds, etc., and are best represented by an envelope. Over the years many pattern models have been suggested for large reflector antennas, see e.g., [5-7].

A simple but effective method of characterizing an actual antenna pattern is to use a model which is based on many theoretical and experimental results and provide an upper- and/or lower-bound or envelope for the antenna which can be easily applied to many situations. Ideally, following the definition of directivity of an antenna, the gain model G given in dB, ignoring the difference between gain and directivity, should obey the formula

$$\int_0^{2\pi}\int_0^{\pi} 10^{\frac{-G(\theta,\phi)}{10}} \sin(\theta)d\theta d\phi = 4\pi \ , \qquad (1)$$

and for a circularly symmetric pattern

$$\int_0^{\pi} 10^{\frac{-G(\theta,\phi)}{10}} \sin(\theta)d\theta = 2 \qquad (2)$$

However, in the models that are usually used, since an upper limit envelope is used for the pattern and not the actual pattern, the value of the integral is much larger. But its value can be used as a sanity check for how close it is to an actual antenna pattern.

Here we consider four different models for high gain ground antennas. The model definitions are then used to evaluate cumulative probability function and probability density function for the gain value at a receiving antenna randomly located anywhere in the far field of the model antenna. The models are all assumed to be circularly symmetric around the boresight axis.

We distinguish two cases for the gain models.

i) A two-dimensional case, in which the model simulate the pattern in a plane cut through the boresight of the antenna and the range of the angle from boresight is assumed to be $0 < \theta < 180°$.

ii) A three-dimensional case, in which the pattern given is anywhere in the half-space above the ground, and the range of the angle from boresight is assumed to be $0 < \theta < 90°$.

Now we proceed with the definition of the models.

1) The first model is a simple standard model commonly used, and is represented as:

$$\begin{aligned} G &= G_0 && 0 < \theta < \theta_1 \\ G &= C_1 - C_2 \log(\theta) && \theta_1 < \theta < \theta_2 \\ G &= C3 && \theta_2 < \theta < \theta_e \\ \theta_e &= 90°, \text{ for 3-D case} \\ \theta_e &= 180°, \text{ for 2-D case} \end{aligned} \qquad (3)$$

with,

$$G_0 = \text{a given peak boresight gain}$$

$$C_1 = \begin{matrix} 32.0, \text{ for D>100}\lambda \text{ (gain>48dB)} \\ 29.3, \text{ for D<100}\lambda \text{ (gain<48dB)} \end{matrix} \ ,$$

$$C_2 = 25, \text{the slope parameter}$$

$$C_3 = \begin{matrix} \text{-10.0, for D>100}\lambda \text{ (gain>48dB)} \\ \text{-12.7, for D<100}\lambda \text{ (gain<48dB)} \end{matrix}$$

and

$$\theta_1 = 10^{(C_1 - C_0)/C_2}$$

$$\theta_2 = 10^{(C_1 - C_3)/C_2}$$

2) The second model is a "smoothed" version of the first model and given as:

$$\begin{aligned} G &= G_0 - a_1(\theta/\theta_1)^2 && 0 < \theta < \theta_1 \\ G &= C_1 - C_2 \log(\theta) && \theta_1 < \theta < \theta_2 \\ G &= C3 + a_2\left(\frac{\theta - \theta_e}{\theta_2 - \theta_e}\right)^{n(n+3)} && \theta_2 < \theta < \theta_e \\ \theta_e &= 90°, n = 1, \text{ for 3-D case} \\ \theta_e &= 180°, n = 2, \text{for 2-D case} \end{aligned} \qquad (4)$$

with,

$$G_0 = \text{a given peak boresight gain}$$

$$C_1 = \begin{matrix} 32.0, \text{ for D>100}\lambda \text{ (gain>48dB)} \\ 29.3, \text{ for D<100}\lambda \text{ (gain<48dB)} \end{matrix} \ ,$$

$$C_2 = 25, \text{the slope parameter}$$

$$C_3 = \begin{matrix} \text{-10.0, for D>100}\lambda \text{ (gain>48dB)} \\ \text{-12.7, for D<100}\lambda \text{ (gain<48dB)} \end{matrix}$$

$$\theta_{10} = 10^{(C_1 - C_0)/C_2},$$
$$\theta_{20} = 10^{(C_1 - C_3)/C_2}$$
$$\theta_1 = \theta_{10}\sqrt{e}$$
$$\theta_2 = \theta_e - (\theta_e - \theta_{20})e^{\frac{1}{2n^2}},$$

and

$$a_1 = \frac{1}{2}\log(e)C_2$$
$$a_2 = C_1 - C_3 - C_2\log(\theta_2)$$

3) The third model is more realistic in terms of the main lobe and near sidelobes and is given by

$$\begin{aligned} G &= G_0 & 0 < \theta < \theta_1 \\ &= C_1 - C_2\log(\theta) & \theta_1 < \theta < \theta_2 \\ &= C3 & \theta_2 < \theta < \theta_e \end{aligned} \quad (5)$$

with

G_0 = a given peak boresight gain

$C_2 = 25$, the slope parameter,

$C_3 = \begin{cases} -10.0, \text{ for } D>100\lambda \text{ (gain>48dB)} \\ -12.7, \text{ for } D<100\lambda \text{ (gain<48dB)} \end{cases}$

$\theta_{hp} = \frac{1}{2}\sqrt{\frac{27000}{10^{G_0/10}}}$, half the 3-dB beamwidth

$$\theta_1 = \frac{1}{\sqrt{e}}\theta_{hp}\sqrt{\frac{\log(e)}{20\log(2)}C_2},$$

$$C_1 = G_0 + C_2\log(\theta_1),$$

and,

$$\theta_2 = 10^{(C_1 - C_3)/C_2}$$

4) This fourth model is a "smoothed" version of the third model and is given as

$$\begin{aligned} G &= G_0 - a_1(\theta/\theta_1)^2 & 0 < \theta < \theta_1 \\ G &= C_1 - C_2\log(\theta) & \theta_1 < \theta < \theta_2 \\ G &= C3 + a_2\left(\frac{\theta - \theta_e}{\theta_2 - \theta_e}\right)^{n(n+5)} & \theta_2 < \theta < \theta_e \end{aligned} \quad (6)$$

$\theta_e = 90°, n = 1$, for 3-D case

$\theta_e = 180°, n = 2$, for 2-D case

with,

G_0 = a given peak boresight gain

$C_2 = 25$, the slope parameter

$C_3 = \begin{cases} -10.0, \text{ for } D>100\lambda \text{ (gain>48dB)} \\ -12.7, \text{ for } D<100\lambda \text{ (gain<48dB)} \end{cases}$

$\theta_{hp} = \frac{1}{2}\sqrt{\frac{27000}{10^{G_0/10}}}$, half the 3-dB beamwidth,

$$\theta_1 = \theta_{hp}\sqrt{\frac{\log(e)}{20\log(2)}C_2}$$

$$a_1 = \frac{1}{2}\log(e)C_2$$

$$C_1 = C_0 + C_2\log(\frac{\theta_1}{\sqrt{e}}),$$

$$\theta_{20} = 10^{(C_1 - C_3)/C_2}$$

$$\theta_2 = \theta_e - (\theta_e - \theta_{20})e^{\frac{2}{(2n+1)^2}},$$

and,

$$a_2 = C_1 - C_3 - C_2\log(\theta_2).$$

Figure 1 shows a comparative plot of all four models for an antenna with a gain of 85 dB (approximately, the 70 meter antenna at 34 GHz frequency), using the 3-D model. Figure 2 shows similar plots, for an antenna with 46 dB gain, using the 2-D model. Notice that in both cases the new model provides a better approximation to the 3-DB beam-width near the boresight than the original model. The 3-dB half beam-widths at 85 and 46 dB gain are approximately 0.0046 and 0.412 degrees, respectively..

3. GAIN PROBABILITY FUNCTIONS

The gain value as seen by a receiver at a random location, exposed to the radiation from a transmitting antenna with a given gain profile, can be thought of as a uniformly distributed random variable (same is true if the receiver is fixed but the transmitting antenna makes a random rotation. The gain pattern is, in general, given by

$$G = G(\theta, \phi), \begin{cases} 0° < \theta < 180° \\ 0° < \phi < 360° \end{cases}$$

Assuming circular symmetry around the boresight axis, only the gain pattern in one cut through the boresight axis is needed and is given by

$$G = G(\theta),\ 0° < \theta < 180°,\ \text{for any } \varphi, 0° < \phi < 360°$$

Here we consider two distinct cases.

I) In a two-dimensional case, the receiver is assumed to be in a plane through the boresight of the antenna. For example, if the transmitting antenna is horizontally directed, then the receiver is also in a horizontal plane around the antenna. In this case, the probability that the gain at the receiver is below a given gain level (the cumulative probability) is given by:

$$P_c(G) = \frac{\int_{\theta(G)}^{\theta_e} d\theta}{\int_0^{\theta_e} d\theta} = \frac{\theta_e - \theta(G)}{\theta_e} \tag{6}$$

or with $\theta_e = 180°$

$$P_c(G) = 1 - \frac{\theta(G)}{180}$$

The probability density function of the gain at the receiver is then given by

$$P(G) = \frac{dP_c(G(\theta))}{dG} = \frac{\partial P_c(G(\theta))}{\partial \theta}\frac{\partial \theta}{\partial G} = \frac{\frac{\partial P_c(G(\theta))}{\partial \theta}}{\frac{\partial G}{\partial \theta}} \tag{7}$$

For the P_c function given above we obtain,

$$P(G) = \frac{-1}{\theta_e G'(\theta)} \tag{8}$$

II) In a three dimensional case, the receiver is assumed to be anywhere in the half-space above the ground and for simplicity, the transmit antenna boresight is considered in the zenith direction normal to the ground plane. However, The results thus obtained are approximately correct even for cases in which the transmit antenna is pointing in an arbitrary direction as long as the antenna is a high gain pencil beam antenna and is pointing at least a few beamwidths above the horizontal ground plane. In this scenario, the probability that the gain at the receiver is below a given gain level (the cumulative probability) is given by:

$$P_c(G) = \frac{\int_0^{360} d\phi \int_{\theta(G)}^{\theta_e} \sin(\theta) d\theta}{\int_0^{360} d\phi \int_0^{\theta_e} \sin(\theta) d\theta} = \frac{\cos(\theta(G)) - \cos(\theta_e)}{1 - \cos(\theta_e)}$$

In which $\theta_e = 90°$ (9)

and results in

$$P_c(G) = \cos(\theta(G)) \tag{10}$$

Following the procedure in the two-dimensional case, the gain probability density function is obtained as

$$P(G) = \frac{dP_c(G(\theta))}{dG} = \frac{\frac{\partial P_c(G(\theta))}{\partial \theta}}{\frac{\partial G}{\partial \theta}} = -\left(\frac{\pi}{180}\right)\frac{\sin(\theta(G))}{G'(\theta)} \tag{11}$$

The factor (π/180) is introduced because the angle arguments in cosine and sine functions are assumed to be in degrees.
Now we are in a position to apply these equations to the gain models developed in the previous section. For the four cases that we developed in that section we obtain the following results. Notice that in each case, reference is made to the parameters C_1, C_2, C_3, a_1, a_2, θ_1, and θ_2 from the respective model definition:

1) The simple original gain model:

2-D case:

$$P_c(G) = \begin{cases} 0, & G < C_3 \\ 1 - \frac{\theta}{180} = 1 - \frac{10^{\frac{C_1 - G}{C_2}}}{180}, & C_3 < G < G_0 \\ 1, & G_0 < G \end{cases} \tag{12}$$

$$\begin{aligned} P(G) &= \left(1 - \frac{\theta_2}{180}\right)\delta(G - G_3) \\ &\quad + \frac{\theta(G)}{180 \cdot \log(e) \cdot C_2} + \frac{\theta_1}{180}\delta(G - G_0) \\ &= \left(1 - \frac{10^{\frac{C_1 - C_3}{C_2}}}{180}\right)\delta(G - G_3) \\ &\quad + \frac{10^{\frac{C_1 - G}{C_2}}}{180 \cdot \log(e) \cdot C_2} \\ &\quad + \frac{10^{\frac{C_1 - G_0}{C_2}}}{180}\delta(G - G_0), \quad G_3 < G < G_0 \end{aligned} \tag{13}$$

3-D case:

$$P_c(G)=\begin{cases} 0, & G<C_3 \\ \cos(\theta)=\cos(10^{\frac{C_1-G}{C_2}}), & C_3<G<G_0 \\ 1, & G_0<G \end{cases} \quad (14)$$

$$\begin{aligned} P(G) &= \cos(\theta_2)\delta(G-G_3) \\ &\quad +(\frac{\pi}{180})\cdot\frac{\theta(G)}{\log(e)\cdot C_2}\cdot\sin(\theta(G)) \\ &\quad +[1-\cos(\theta_1)]\delta(G-G_0) \\ &= \cos(10^{\frac{C_1-C_3}{C_2}})\delta(G-G_3) \\ &\quad +(\frac{\pi}{180})\cdot\frac{10^{\frac{C_1-G}{C_2}}}{\log(e)\cdot C_2}\cdot\sin(10^{\frac{C_1-G}{C_2}}) \\ &\quad +[1-\cos(10^{\frac{C_1-G_0}{C_2}})]\delta(G-G_0), \quad G_3<G<G_0 \end{aligned} \quad (15)$$

2) The interpolated original gain model:

2-D case:

$$P_c(G)=\begin{cases} 1-\frac{1}{180}[180-(180-\theta_2)(\frac{G-G_3}{a_2})^{\frac{1}{10}}], \\ \qquad C_3<G<C_3+a_2 \\ 1-\frac{\theta}{180}, \\ \qquad C_3+a_2<G<G_0-a_1 \\ \frac{\theta_1}{180}\sqrt{\frac{G_0-G}{a_1}}, \\ \qquad G_0-a_1<G<G_0 \end{cases} \quad (16)$$

$$P(G)=\begin{cases} \frac{(180-\theta_2)(G-G_3)^{(\frac{1}{10}-1)}}{180\cdot 10\cdot a_2^{\frac{1}{10}}}, & G_3<G<G_3+a_2 \\ \frac{10^{\frac{C_1-G}{C_2}}}{180\cdot\log(e)\cdot C_2}, & G_3+a_2<G<G_0-a_1 \\ \frac{\theta_1}{180\cdot\sqrt{4a_1(G_0-G)}}, & G_0-a_1<G<G_0 \end{cases} \quad (17)$$

3-D case:

$$P_c(G)=\begin{cases} \cos\left(90+(\theta_2-90)(\frac{G-G_3}{a_2})^{\frac{1}{4}}\right), \\ \qquad C_3<G<C_3+a_2 \\ \cos(\theta)=\cos\left(10^{\frac{C_1-G}{C_2}}\right), \\ \qquad C_3+a_2<G<G_0-a_1 \\ cos\left(\theta_1\sqrt{\frac{G_0-G}{a_1}}\right), \\ \qquad G_0-a_1<G<G_0 \end{cases} \quad (18)$$

$$P(G)=\begin{cases} (\frac{\pi}{180})\cdot\frac{(90-\theta_2)(G-G_3)^{\frac{1}{4}-1}}{4a_2^{\frac{1}{4}}}\cdot \\ \sin\left(90-(90-\theta_2)(\frac{G-G_3}{G2})^{\frac{1}{4}}\right), \\ \qquad G_3<G<G_3+a_2 \\ (\frac{\pi}{180})\cdot\frac{10^{\frac{C_1-G}{C_2}}}{C_2\log(e)}\cdot\sin(10^{\frac{C_1-G}{C_2}}), \\ \qquad G_3+a_2<G<G_0-a_1 \\ (\frac{\pi}{180})\cdot\frac{\theta_1}{\sqrt{4a_1(G_0-G)}}\cdot \\ \sin\left(\theta_1\sqrt{\frac{G_0-G}{a_1}}\right), \\ \qquad G_0-a_1<G<G_0 \end{cases} \quad (19)$$

3) The simple new model: The forms of the equations for this case are identical to the ones for the original model (case 1). The only difference is in the definition of the parameters C_1, θ_1, and θ_2.

4) The interpolated new gain model:

2-D case:

$$P_c(G)=\begin{cases} 1-\frac{1}{180}[180-(180-\theta_2)(\frac{G-G_3}{a_2})^{\frac{1}{16}}], \\ \qquad C_3<G<C_3+a_2 \\ 1-\frac{\theta}{180}, \\ \qquad C_3+a_2<G<G_0-a_1 \\ 1-\frac{\theta_1}{180}\sqrt{\frac{G_0-G}{a_1}}, \\ \qquad G_0-a_1<G<G_0 \end{cases} \quad (20)$$

$$P(G)=\begin{cases}\dfrac{(180-\theta_2)(G-G_3)^{(\frac{1}{16}-1)}}{180\cdot 16\cdot a_2^{\frac{1}{16}}}, & G_3<G<G_3+a_2\\[2ex] \dfrac{10^{\frac{C_1-G}{C_2}}}{180\cdot\log(e)\cdot C_2}, & G_3+a_2<G<G_0-a_1\\[2ex] \dfrac{\theta_1}{180\cdot\sqrt{4a_1(G_0-G)}}, & G_0-a_1<G<G_0\end{cases} \quad (21)$$

3-D case:

$$P_c(G)=\begin{cases}\cos\left[90+(\theta_2-90)(\dfrac{G-G_3}{a_2})^{\frac{1}{7}}\right], & C_3<G<C_3+a_2\\[2ex] \cos(\theta)=\cos(10^{\frac{C_1-G}{C_2}}), & C_3+a_2<G<G_0-a_1\\[2ex] cos\left(\theta_1\sqrt{\dfrac{G_0-G}{a_1}}\right), & G_0-a_1<G<G_0\end{cases} \quad (22)$$

$$P(G)=\begin{cases}\dfrac{\pi}{180}\cdot\dfrac{(90-\theta_2)(G-G_3)^{\frac{1}{7}-1}}{7a_2^{\frac{1}{7}}}\cdot \sin\left(90-(90-\theta_2)(G-G_3)^{\frac{1}{7}}\right), & G_3<G<G_3+a_2\\[2ex] \dfrac{\pi}{180}\cdot\dfrac{10^{\frac{C_1-G}{C_2}}}{C_2\log(e)}\cdot\sin(10^{\frac{C_1-G}{C_2}}), & G_3+a_2<G<G_0-a_1\\[2ex] \dfrac{\pi}{180}\cdot\dfrac{\theta_1}{\sqrt{4a_1(G_0-G)}}\cdot\sin\left(\theta_1\sqrt{\dfrac{G_0-G}{a_1}}\right), & G_0-a_1<G<G_0\end{cases} \quad (23)$$

Figures 3 through 10 show the gain models and their associated cumulative probability functions and probability density functions. The probability density functions for the non-interpolated models have impulse responses both at the beginning and the end points for both the 2-D as well as 3-D cases. In the interpolated cases, however, there are no impulse functions, but the function goes to infinity at both the beginning and end points for the 2-D cases, and only at the beginning points for 3-D cases.

4. Summary and Conclusions

In this paper we have derived closed form expressions for the DSN antenna gain density function and the cumulative gain probability function using modeled 2-D and 3-D gain patterns. These functions can be used to assess the effect of HDFS transmitters on the DSN. They can also be used to determine the necessary coordination distance that these transmitters must be away from the DSN antennas in order to protect the DSN.

Acknowledgment

The research described in this paper was carried out at the Jet Propulsion Laboratory, California Institute of Technology, under a contract with the National Aeronautics and Space Administration. The author would like to acknowledge the kind encouragement and helpful suggestions of Miles Sue of JPL. The efforts of Charles Ruggier, Daniel Bathker, Peter Kinman, and Ted Peng in various activities leading to the preparation of this manuscript are also appreciated.

References

[1] "Elements of a Methodology to Estimate the Global Distribution of Potential Hub Stations of Point-to-Multipoint Fixed Service Systems," contributed by USA, Document 7D-9D/36-E, ITU-R, 1998.

[2] C. Ho, M. Sue, and C. Ruggier, "An Estimate of Interference Effect From the Los Angeles Area High-Density Fixed Services (HDFS) on the Goldstone DSN Receiver Above 30 GHz: Monte Carlo Simulation," JPL TMO Progress Report 42-138, August 15, 1999.

[3] C. Ho, M. Sue, T. Peng, P. Kinman, and H. Tan, "Interference Effects of Deep Space Network Transmitters on IMT-2000/UMTS Receivers at S-Band," JPL TMO Progress Report 42-142, April-June, 2000.

[4] C. Ho, D. Bathker, M. Sue, and T. Peng, " Adjacent Band Interference from San Diego Area Transmitters to Goldstone Deep Space Network Receivers Near 2300 Megahertz," JPL TMO Progress Report 42-142, October-December 2001.

[5] "Mathematical Model of Average and Related Radiation Patterns for Line-of-Sight Point-to-Point Radio-Relay System Antennas for Use in Certain Coordination Studies and Interference Assessment in the Frequency Range from 1 GHz
to about 70 GHz," Recommendation ITU-R F.1245-1, ITU-R, 2000.

[6] "Generalized Space Research Earth Station And Radio Astronomy Antenna Radiation Pattern For Use In

Interference Calculations, Including Coordination Procedures," Recommendation ITU-R SA.509-2, 1978-1998.

[7] "Methods For Predicting Radiation Patterns Of Large Antennas Used For Space Research And Radio Astronomy," Recommendation ITU-R SA. 1345, 1998.

Vahraz Jamnejad *is a principal engineer at the Jet Propulsion Laboratory, California Institute of Technology. He received his M.S. and Ph.D. in electrical engineering from the University of Illinois at Urbana-Champaign, specializing in electromagnetics and antennas. At JPL, he has been engaged in research and software and hardware development in various areas of spacecraft antenna technology and satellite communication systems. Among other things, he has been involved in the study, design, and development of ground and spacecraft antennas for future generations of Land Mobile Satellite Systems at L band, Personal Access Satellite Systems at K/Ka band, as well as feed arrays and reflectors for future planetary missions. His latest work on communication satellite systems involved the development of ground mobile antennas for K/Ka band mobile terminal, for use with ACTS satellite system. In the past few years, he has been active in research in parallel computational electromagnetics as well as in developing antennas for MARS sample return orbiter. More recently he has studied the applicability of large arrays of small aperture reflector antennas for the NASA Deep Space Network, and is presently active in the preliminary design of a prototype array for this application. Over the years, he has received many US patents and NASA certificates of recognition.*

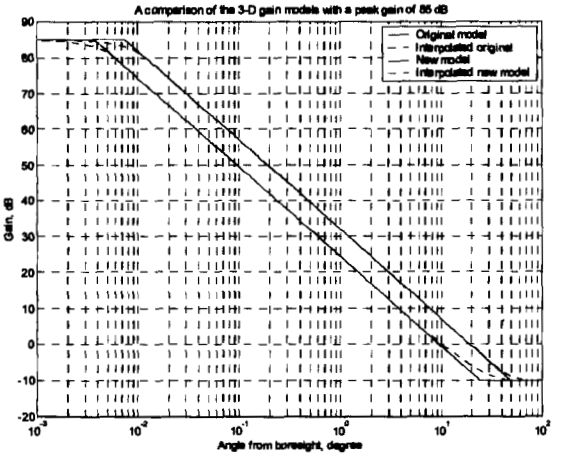

Figure 1. A comparison of 3-D gain models for a 85 dB gain antenna.

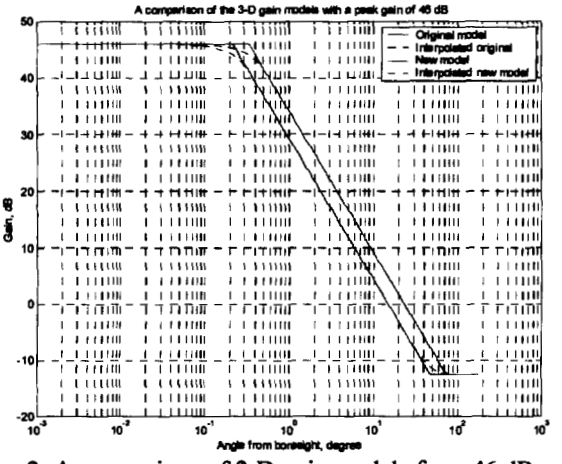

Figure 2. A comparison of 2-D gain models for a 46 dB gain antenna.

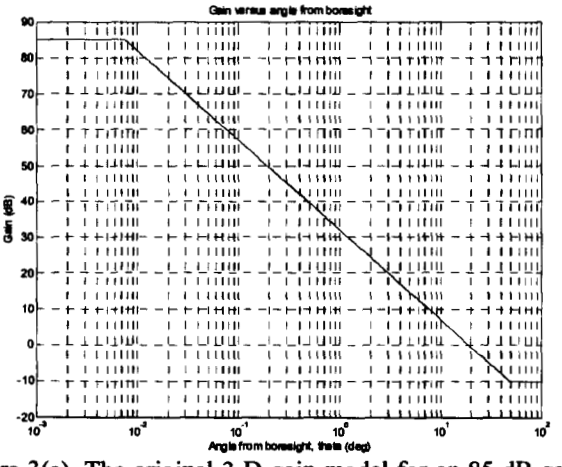

Figure 3(a). The original 3-D gain model for an 85-dB gain antenna

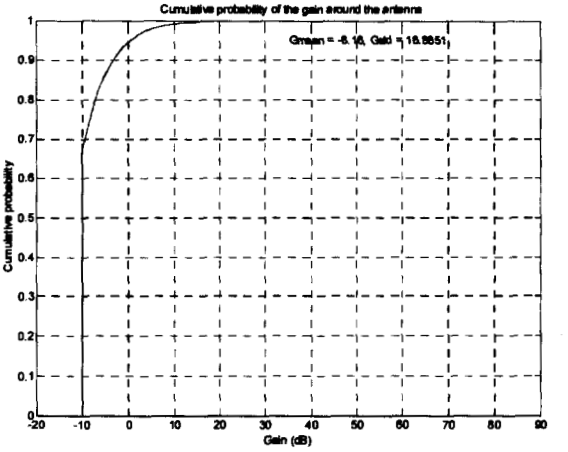

Figure 3(b). The cumulative probability function for the original 3-D gain model of an 85-dB gain antenna.

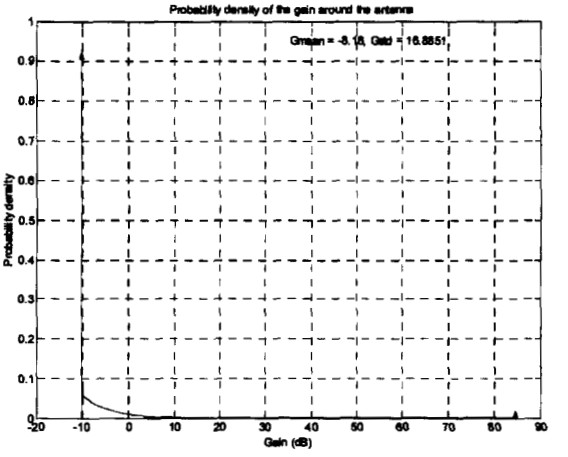

Figure 3(c). The probability density function for the original 3-D gain model of an 85-dB gain antenna .

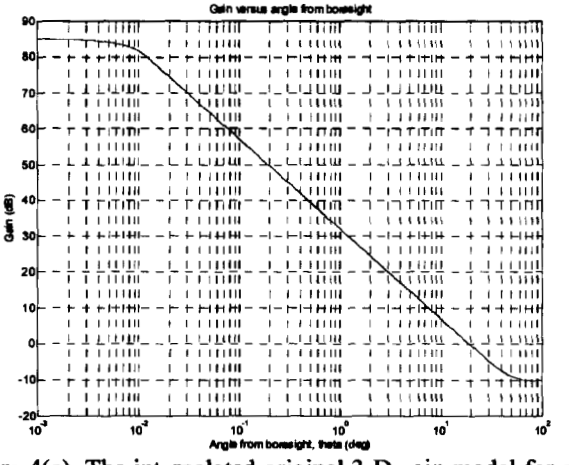

Figure 4(a). The interpolated original 3-D gain model for an 85-dB gain antenna.

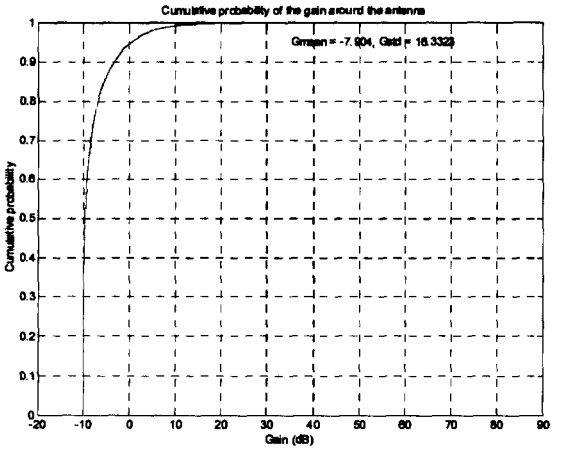

Figure 4(b). The cumulative probability function for the interpolated original 3-D gain model of an 85-dB gain antenna.

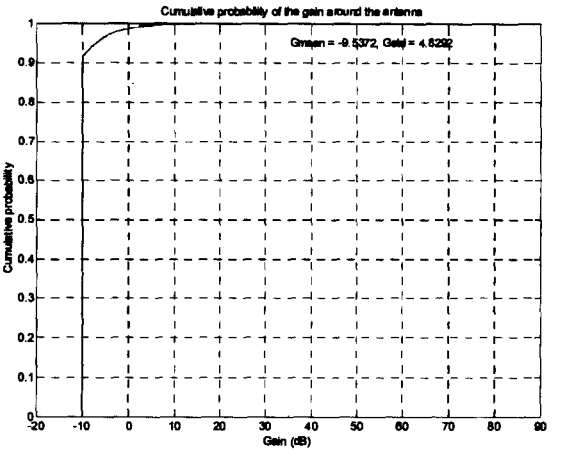

Figure 5(b). The cumulative probability function for the new 3-D gain model of an 85-dB gain antenna.

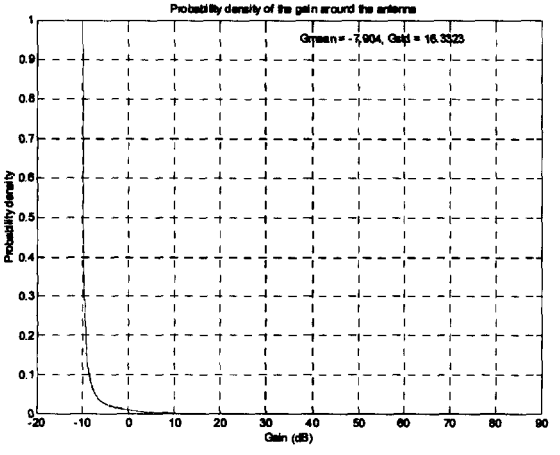

Figure 4(c). The probability density function for the interpolated original 3-D gain model of an 85-dB gain antenna.

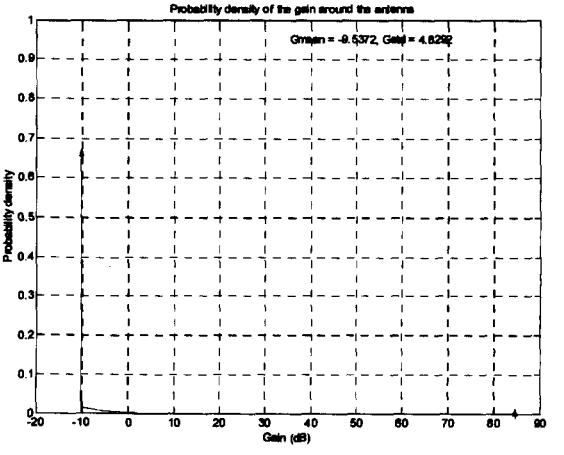

Figure 5(c). The probability density function for the new 3-D gain model of an 85-dB gain antenna.

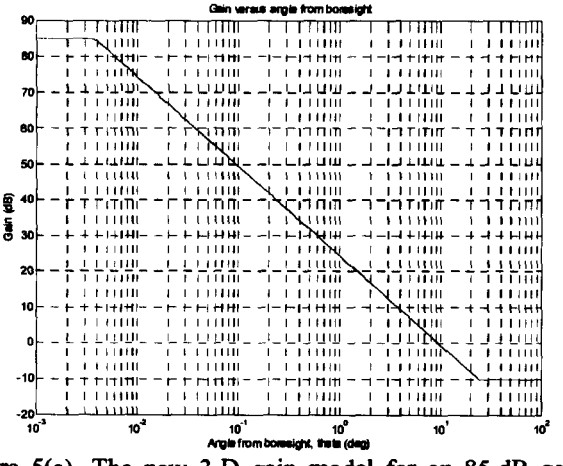

Figure 5(a). The new 3-D gain model for an 85-dB gain antenna.

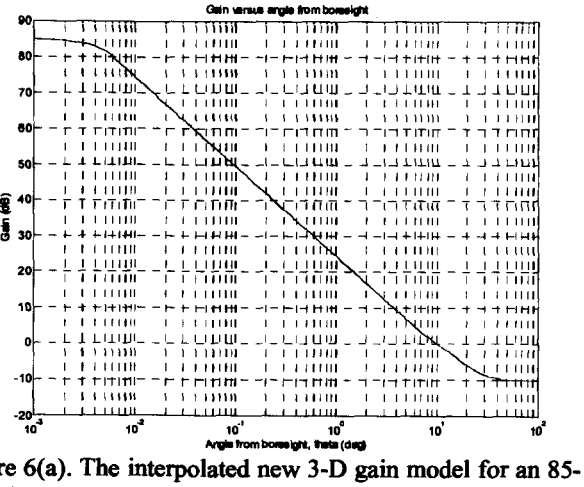

Figure 6(a). The interpolated new 3-D gain model for an 85-dB gain antenna.

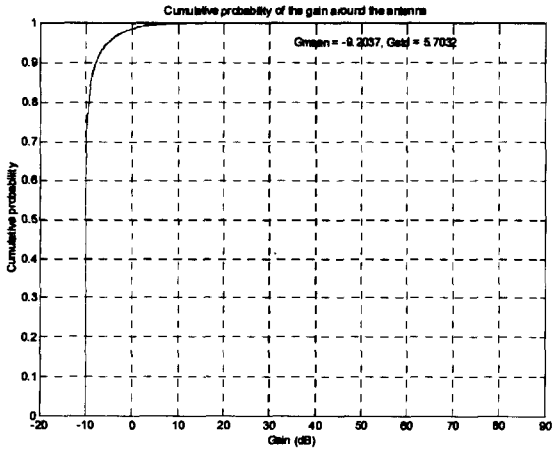

Figure 6(b). The cumulative probability function for the interpolated new 3-D gain model of an 85-dB gain antenna.

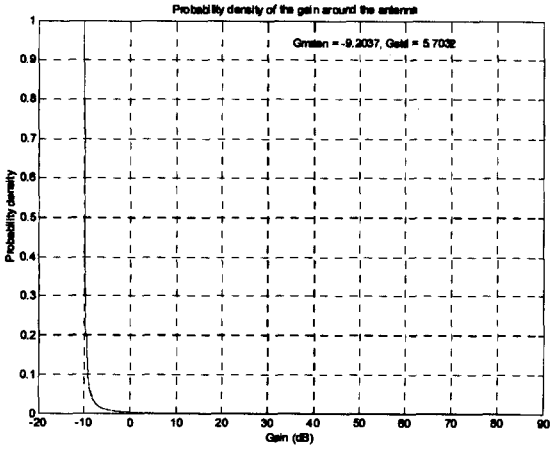

Figure 6(c). The probability density function for the interpolated new 3-D gain model of an 85-dB gain antenna.

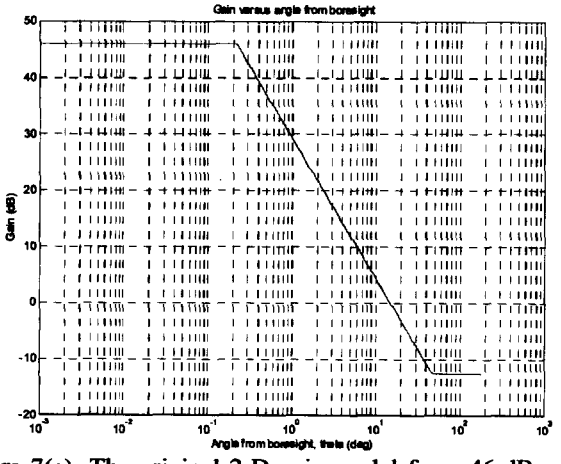

Figure 7(a). The original 2-D gain model for a 46-dB gain antenna.

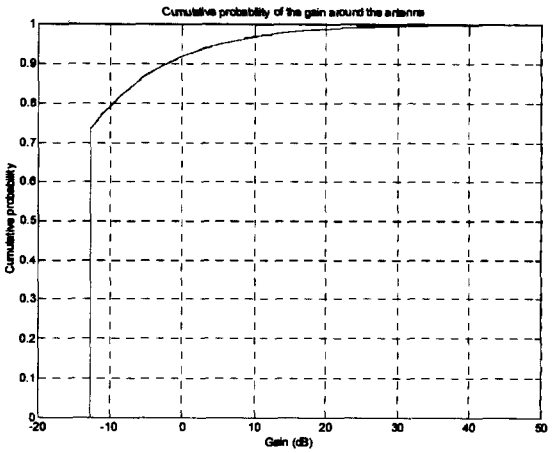

Figure 7(b). The cumulative probability function for the original 2-D gain model of a 46-dB gain antenna.

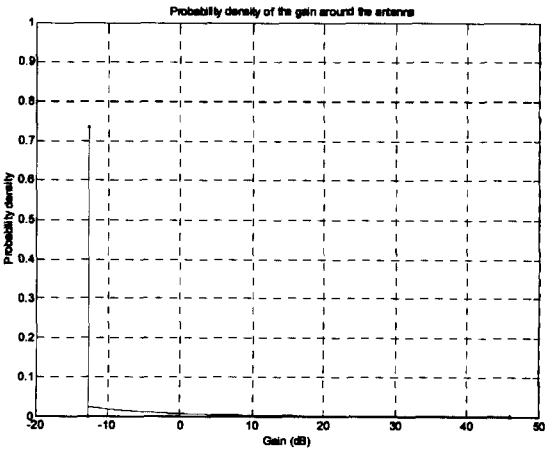

Figure 7(c).The probability density function for the original 2-D gain model of a 46-dB gain antenna.

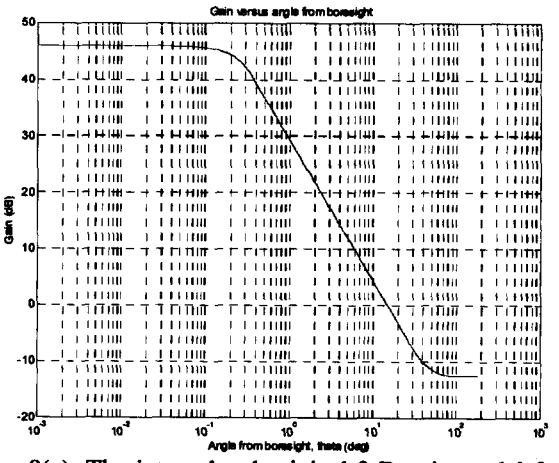

Figure 8(a). The interpolated original 2-D gain model for a 46-dB gain antenna.

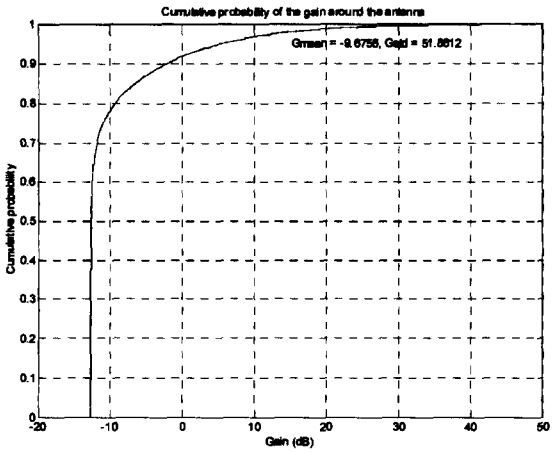

Figure 8(b). The cumulative probability function for the interpolated original 2-D gain model of a 46-dB gain antenna.

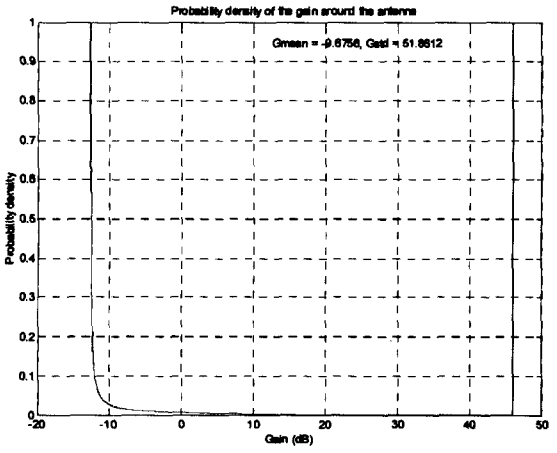

Figure 8(c). The probability density function for the interpolated original 2-D gain model of a 46-dB gain antenna.

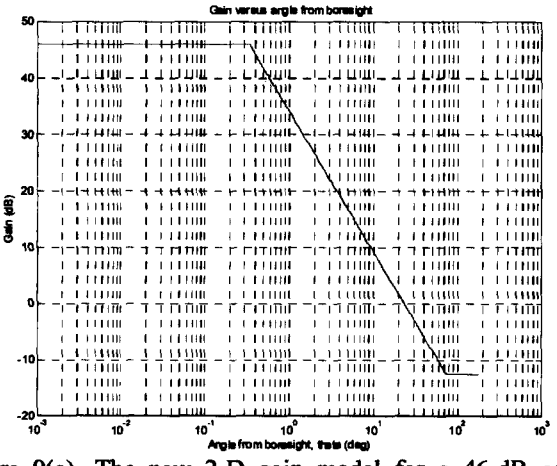

Figure 9(a). The new 2-D gain model for a 46-dB gain antenna.

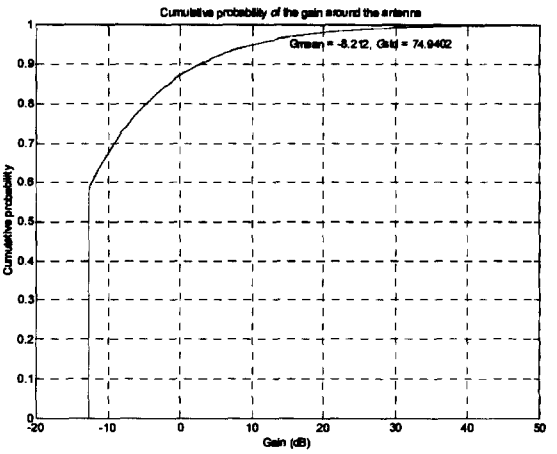

Figure 9(b). The cumulative probability function for the new 2-D gain model of a 46-dB gain antenna.

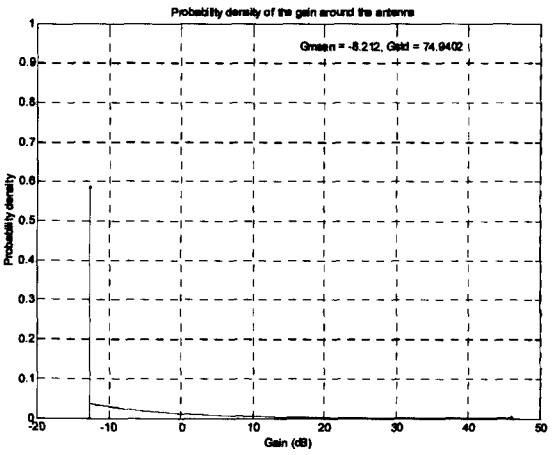

Figure 9(c). The probability density function for the new 2-D gain model of a 46-dB gain antenna.

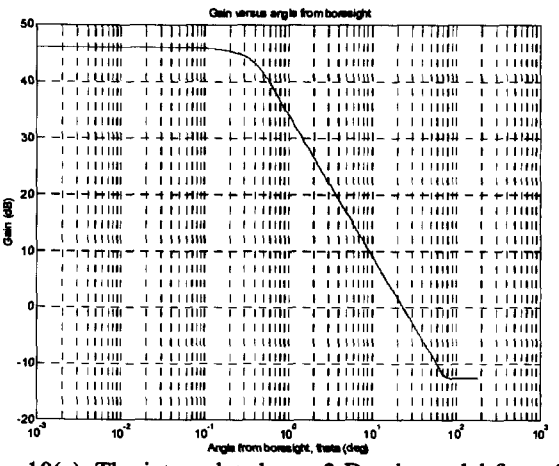

Figure 10(a). The interpolated new 2-D gain model for a 46-dB gain antenna.

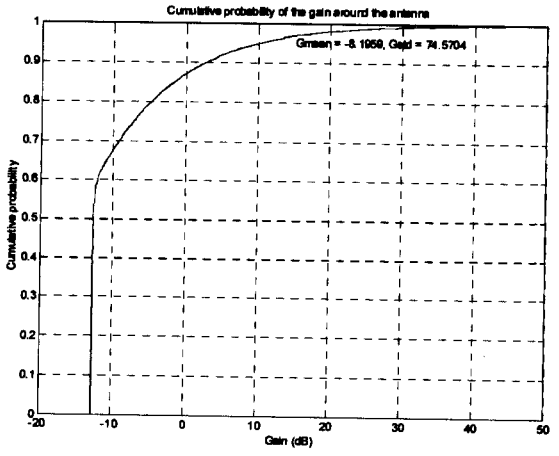

Figure 10(b). The cumulative probability function for the interpolated new 2-D gain model of a 46-dB gain antenna.

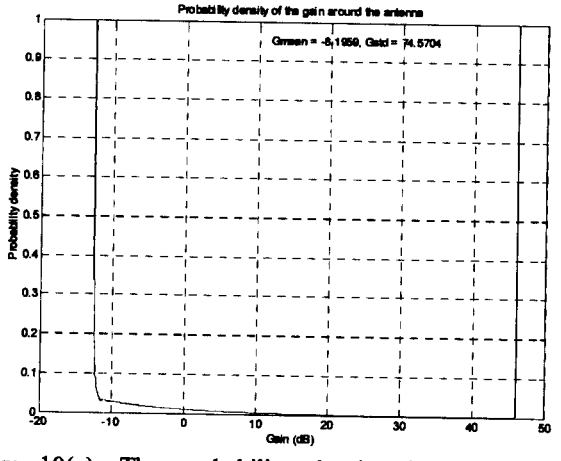

Figure 10(c). The probability density function for the interpolated new 2-D gain model of a 46-dB gain antenna.